Insights into the dose-response relationship of radioembolization with resin yttrium-90 microspheres: a prospective cohort study in patients with colorectal cancer liver metastases

Andor F. van den Hoven *et al.*

This supplemental data document provides information about the validation process of the method for quantitative ^{90}Y-PET analyses and the linear mixed effects regression model used in our study.

Background

Quantitative analyses of the posttreatment ^{90}Y-activity distribution after radioembolization have been challenging due to the lack of positron and γ-ray emission. The first method to become available was the detection of secondary γ-rays, a product of bremsstrahlung, on SPECT. Unfortunately, bremsstrahlung SPECT proved to be of little clinical value for dose quantification in small tumors (< 2-3 cm), due to its limited spatial resolution and high scatter. Nowadays, the quantitative accuracy of bremsstrahlung SPECT can be improved by specialized reconstruction algorithms, as demonstrated in previous phantom studies (*1,2*), but this is computationally intensive and not widely available in clinical practice. The acknowledgement that the ^{90}Y-activity distribution can also be quantified on PET, utilizing the naturally occurring phenomenon of internal-pair production (*3-5*), sparked a renewed interest in ^{90}Y imaging. (*6,7*) Since then, an abundance of scientific evidence has shown that quantification of ^{90}Y-absorbed doses on PET is valid (*6,8-9*), superior to bremsstrahlung SPECT (10-12), and accurate enough for clinical practice (*13-16*).

So far, no commercial software package has been specifically developed and validated for quantitative analyses of ^{90}Y-PET images. We used ROVER software (ABX GmBH, Radeberg, Germany) for this purpose. This software was originally developed and validated for quantitative analysis of ^{18}F-FDG-PET scans, allowing for threshold-based automatic tumor delineation and partial volume correction. (*17-20*) It also enables co-registration of different scans and ROI transfers between them, so that tumors can be identified on ^{18}F-FDG-PET and absorbed doses can be determined in the same locations on ^{90}Y-PET. Slight differences between ^{18}F and ^{90}Y quantification are to be expected, mainly due to extremely low positron abundance of ^{90}Y (32 x 10^{-6} versus 0.98 for ^{18}F). In a recent phantom study, it was demonstrated that quantification of ^{90}Y-activity in spheres with a diameter of 10 – 30 mm on PET was similar when using ROVER or three other software packages. (*21*)

Validation of ^{90}Y-PET analyses: Phantom experiments

To validate our ^{90}Y-PET measurements, phantom experiments were performed and analyzed with ROVER. First, a cylindrical phantom with a capacity of 6266 g was filled with a hydrochloric acid solution (concentration 1M), and 3.09 GBq of ^{90}Y citrate. The total ^{90}Y activity in the phantom was measured with the same dose calibrator as used in clinical radioembolization procedures to confirm the activity at starting point. Subsequently, PET-images of this phantom were acquired directly after filling the phantom and at four different time points. Finally, the ^{90}Y-PET images were analyzed in ROVER to determine the recovered activity by drawing a total phantom ROI. These measurements were then compared to the real activity at the different time points, as calculated by the decay curve of ^{90}Y (T½ = 64 hours). An excellent correlation (R^2 = 0.999) was found between the PET measurements and actual activity from dose calibration (Supplemental Table 1, Supplemental Fig. 1). Compared with the actual activity, recovered activity measures showed a maximum error of -4.7% down to an activity of 500 kBq/ml, which supports the validity of the ^{90}Y PET acquisitions and analyses in ROVER.

Supplemental Table 1: Difference between the actual ^{90}Y activity in the phantom and the activity recovered on ^{90}Y-PET

Time	Actual activity (MBq)	Recovered activity (MBq)	Recovered - Actual activity (% error)
T0	3089	3038	- 51 (-1.7%)
0.01*T½	3069	2924	-145 (-4.7%)
1.89*T½	835	807	-29 (-3.4%)
2.26*T½	645	628	-18 (-2.8%)
2.62*T½	500	515	+15 (+ 3%)

For five different time points, the actual and recovered ^{90}Y activity are given in MBq. The percentage of error is calculated as follows: (recovered – actual activity)/actual activity * 100. T½ = half-life.

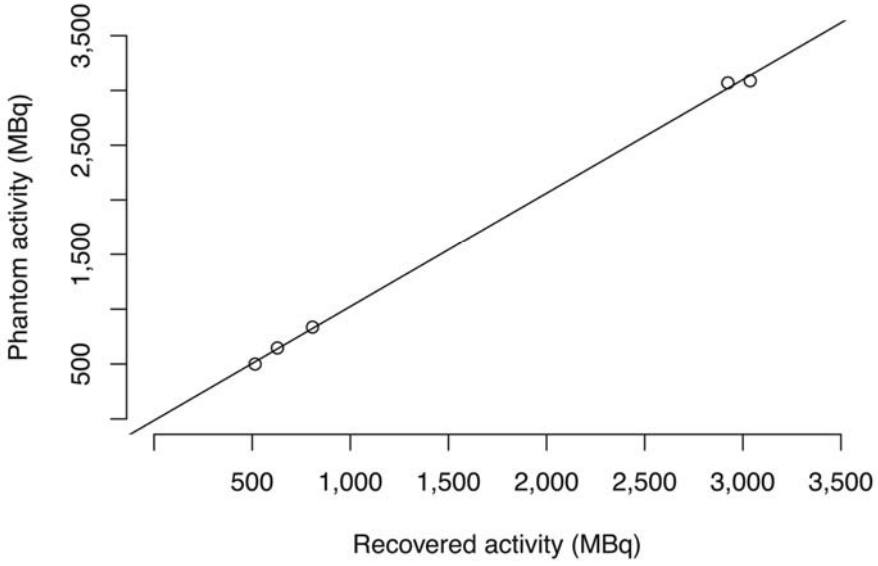

Supplemental Fig. 1: Scatterplot showing a linear relationship between ^{90}Y-PET recovered activity measures and the actual activity in a 6266 g cylindrical phantom filled with a hydrochloric acid ^{90}Y-citrate solution, at five different time points. This relationship can be described by: Actual activity (MBq) = -13.38 MBq + 1.04 x Recovered activity. The correlation was excellent ($R^2 = 0.999$). Compared with the actual activity, recovered activity measures showed a maximum error of -4.7% down to an activity of 500 kBq/ml.

Validation of ^{90}Y-PET analyses: Clinical patients

As an extra validation step, net administered ^{90}Y activity at time of scanning was compared with the recovered ^{90}Y-PET activity in the liver. The net administered ^{90}Y activity at the time of scanning was calculated by subtracting the residual activity in the administration vial (measured by the dose calibrator) from the prepared activity corrected for the radioactive decay between administration and the scan. To determine the recovered ^{90}Y-PET activity, a mask was placed over the entire liver (slightly extending across all edges), and the total activity within this mask was determined in Bq.

A strong correlation and fair agreement was found between the mean ^{90}Y-PET recovered liver activity and the mean administered activity at scan time (Supplemental Figs. 2 and 3). A small overestimation of the administered activity may be attributable to scatter detection at the liver-lung surface, which was avoided in tumor absorbed dose quantification. Thus, quantitative ^{90}Y-PET analyses were considered accurate.

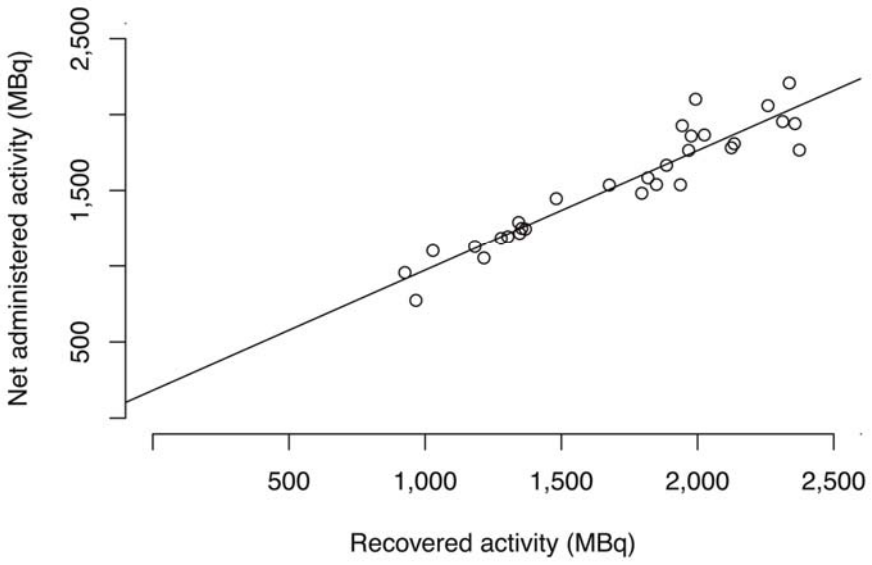

Supplemental Fig. 2: Scatterplot showing a linear relationship between recovered whole liver activity on ^{90}Y-PET and the net administered activity at time of the scan in all 30 patients. This relationship can be described by: *Activity at scan time (MBq) = 199 MBq + 0.78 x Recovered liver activity.*

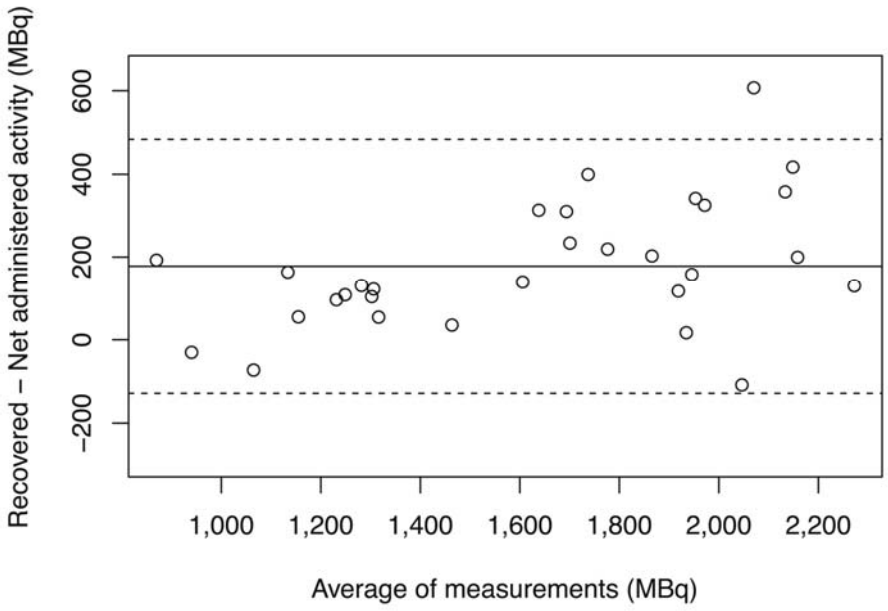

Supplemental Fig. 3: Bland-Altman plot showing a fair agreement between recovered whole liver activity on ^{90}Y-PET and the net administered activity at time of the scan (95% limits of agreement: -140 – 482 MBq). The recovered ^{90}Y-activity measurements overestimate the net administered activity, with increasing overestimation for higher activities. This may be explained by scatter detection at the liver-lung surface.

Linear mixed effects regression model

A linear mixed effects regression (LMER) model was fitted to evaluate the relationship between tumor absorbed dose and posttreatment TLG* at 1m FU, adjusted for baseline TLG*, on a per-lesion basis.

The mixed model accounted for within patient clustering by random intercept. (*22*) We anticipated that the effect of tumor absorbed dose on 1m TLG* may depend on the baseline TLG*, and therefore included an interaction term (Dose:Baseline TLG*). An analysis of variance method with a Chi-square test was used to compare nested models and generate p-values for the fixed effects.

To fulfill model assumptions, posttreatment TLG* was logarithmically transformed. To take potential non-linear relations between dose and baseline TLG* with posttreatment log(TLG*+8) into account, we first evaluated transformations of these variables and selected the transformations providing the lowest Aikaike's Information Criteria value for a model containing these variables and their interaction. The top 10% of baseline TLG* values were truncated before these analyses to prevent inappropriate influential points.

The model explained variance, with and without random intercept, was assessed with R^2 for mixed effects models.(*23*)

The model-derived relation between dose and metabolic response and its dependency on baseline TLG* was graphically displayed (including 95% confidence interval lines) after back transformation of all involved variables to their original scale.

The package 'lme4' (version 1.1-7) was used for LMER modeling in R version 3.1.2.

References

1. Minarik D, Sjögreen Gleisner K, Ljungberg M. Evaluation of quantitative (90)Y SPECT based on experimental phantom studies. *Phys Med Biol*. 2008;53:5689-5703.
2. Rong X, Du Y, Ljungberg M, Rault E, Vandenberghe S, Frey EC. Development and evaluation of an improved quantitative (90)Y bremsstrahlung SPECT method. *Med Phys*. 2012;39:2346-2358.
3. Gates VL, Esmail A a H, Marshall K, Spies S, Salem R. Internal pair production of 90Y permits hepatic localization of microspheres using routine PET: proof of concept. *J Nucl Med*. 2011;52:72-76.
4. D'Arienzo M. Emission of β+ particles via internal pair production in the 0+ – 0+ transition of 90Zr: historical background and current applications in nuclear medicine imaging. *Atoms*. 2013;1:2-12.
5. Lhommel R, Van Elmbt L, Goffette P, et al. Feasibility of 90Y TOF PET-based dosimetry in liver metastasis therapy using SIR-Spheres. *Eur J Nucl Med Mol Imaging*. 2010;37:1654-1662.
6. Pasciak AS, Bourgeois AC, Bradley YC. A Comparison of techniques for (90)Y PET/CT image-based dosimetry following radioembolization with resin microspheres. *Front Oncol*. 2014;4:121.
7. Carlier T, Eugène T, Bodet-Milin C, et al. Assessment of acquisition protocols for routine imaging of Y-90 using PET/CT. *EJNMMI Res*. 2013;3:11.
8. Attarwala AA, Molina-Duran F, Büsing K-A, et al. Quantitative and qualitative assessment of yttrium-90 PET/CT imaging. *PLoS One*. 2014;9:e110401.
9. Martí-Climent JM, Prieto E, Elosúa C, et al. PET optimization for improved assessment and accurate quantification of (90)Y-microsphere biodistribution after radioembolization. *Med Phys*. 2014;41:092503.
10. Padia S a, Alessio A, Kwan SW, Lewis DH, Vaidya S, Minoshima S. Comparison of positron emission tomography and bremsstrahlung imaging to detect particle distribution in patients undergoing yttrium-90 radioembolization for large hepatocellular carcinomas or associated portal vein thrombosis. *J Vasc Interv Radiol*. 2013;24:1147-1153.
11. Lam MGEH, Wondergem M, Elschot M, Smits MLJ. Reply: A clinical dosimetric perspective uncovers new evidence and offers new insight in favor of 99mTc-macroaggregated albumin for predictive dosimetry in 90Y resin microsphere radioembolization. *J Nucl Med*. 2013;54:2192-2193.
12. Zade A a, Rangarajan V, Purandare NC, et al. 90Y microsphere therapy: does 90Y PET/CT imaging obviate the need for 90Y bremsstrahlung SPECT/CT imaging? *Nucl Med Commun*. 2013;34:1090-1096.
13. Chang TT, Bourgeois AC, Balius AM, Pasciak AS. Treatment modification of yttrium-90 radioembolization based on quantitative positron emission tomography/CT imaging. *J Vasc Interv Radiol*. 2013;24:333-337.
14. Kao Y-H, Steinberg JD, Tay Y-S, et al. Post-radioembolization yttrium-90 PET/CT - part 2: dose-response and tumor predictive dosimetry for resin microspheres. *EJNMMI Res*. 2013;3:57.
15. Lea WB, Tapp KN, Tann M, Hutchins GD, Fletcher JW, Johnson MS. Microsphere localization and dose quantification using positron emission tomography/CT following hepatic intraarterial radioembolization with yttrium-90 in patients with advanced hepatocellular carcinoma. *J Vasc Interv Radiol*. 2014;25:1595-1603.

16. D'Arienzo M, Filippi L, Chiaramida P, et al. Absorbed dose to lesion and clinical outcome after liver radioembolization with 90Y microspheres: a case report of PET-based dosimetry. *Ann Nucl Med*. 2013;27:676-680.

17. Torigian D a, Lopez RF, Alapati S, et al. Feasibility and performance of novel software to quantify metabolically active volumes and 3D partial volume corrected SUV and metabolic volumetric products of spinal bone marrow metastases on 18F-FDG-PET/CT. *Hell J Nucl Med*. 2011;14:8-14.

18. Hofheinz F, Pötzsch C, Oehme L, et al. Automatic volume delineation in oncological PET. Evaluation of a dedicated software tool and comparison with manual delineation in clinical data sets. *Nuklearmedizin*. 2012;51:9-16.

19. Hofheinz F, Langner J, Petr J. A method for model-free partial volume correction in oncological PET. *EJNMMI Res*. 2012;2:1-16.

20. Hofheinz F, Langner J, Petr J, et al. An automatic method for accurate volume delineation of heterogeneous tumors in PET. *Med Phys*. 2013;40:082503.

21. Bailey DL. A multicentre comparison of quantitative 90 Y PET / CT for dosimetric purposes after radioembolization with resin microspheres. *EJNMMI*. 2015;42:1202-1222.

22. Casals M, Girabent-Farrés M, Carrasco JL. Methodological quality and reporting of generalized linear mixed models in clinical medicine (2000–2012): A Systematic Review. *PLoS One*. 2014;9:e112653.

23. Johnson PCD. Extension of Nakagawa & Schielzeth's R 2 GLMM to random slopes models. *Methods Ecol Evol*. 2014.